

# Improving MCUCN Code to Simulate Ultracold Neutron Storage and Transportation in Superfluid $^4\text{He}$

INP 2024, April 9<sup>th</sup>, 2024

Xuefen Han, Tiancheng Yi, Songlin Wang

Superadvisor: Prof. Tianjiao Liang

China Spallation Neutron Source (CSNS), Dongguan, China

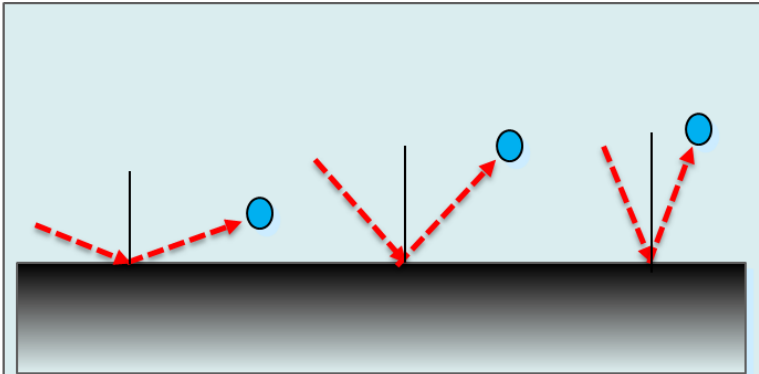
Institute of High Energy Physics (IHEP)

Chinese Academy of Science (CAS)

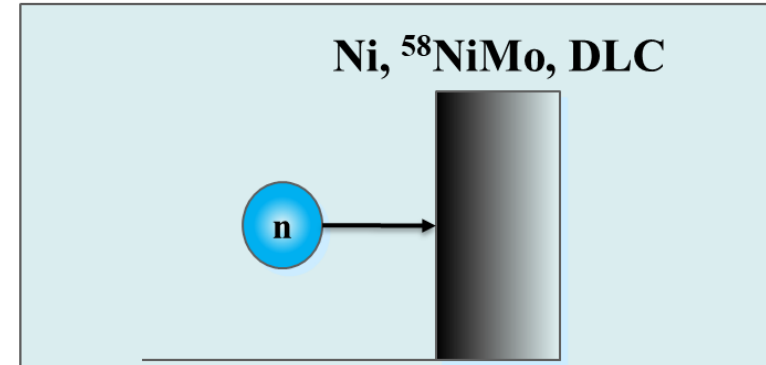


1. **Background of UCN**
2. Physical model enhancement and flow of iMCUCN
3. Comparison of MCUCN, iMCUCN, and UCNtransport
4. Comparison of MCUCN, iMCUCN, and experimental results

Definition:  $E_k < 300 \text{ neV}$ ,  $v < 8 \text{ m/s}$  or  $T < 3 \text{ mK}$

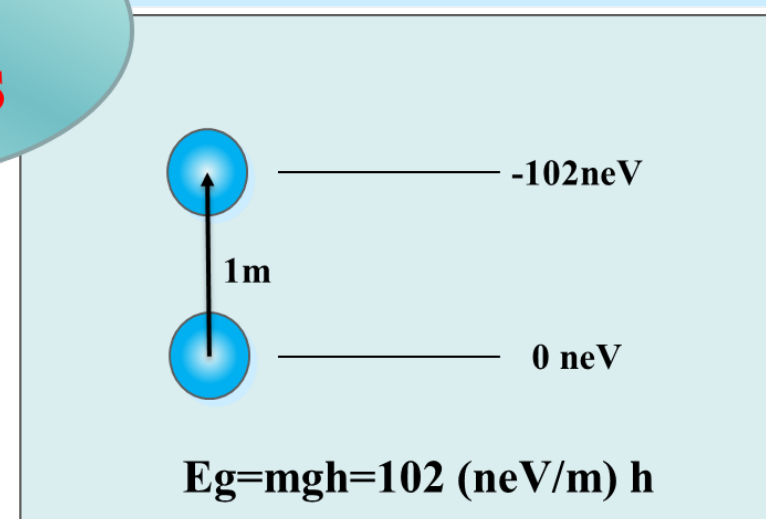
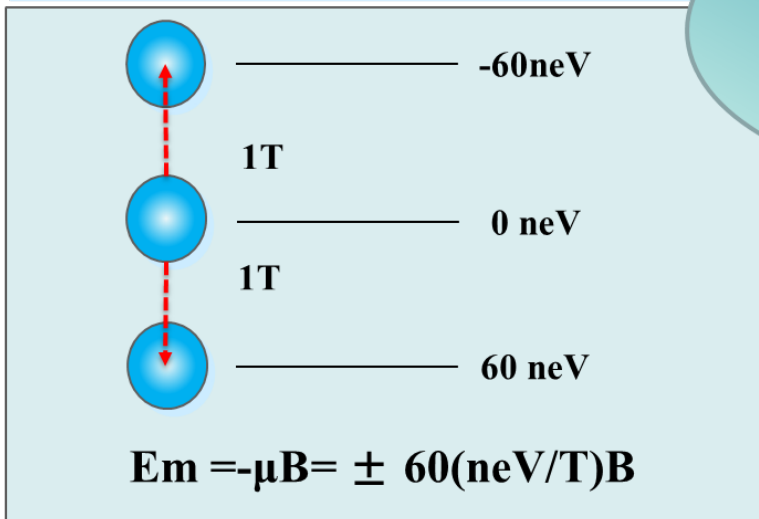


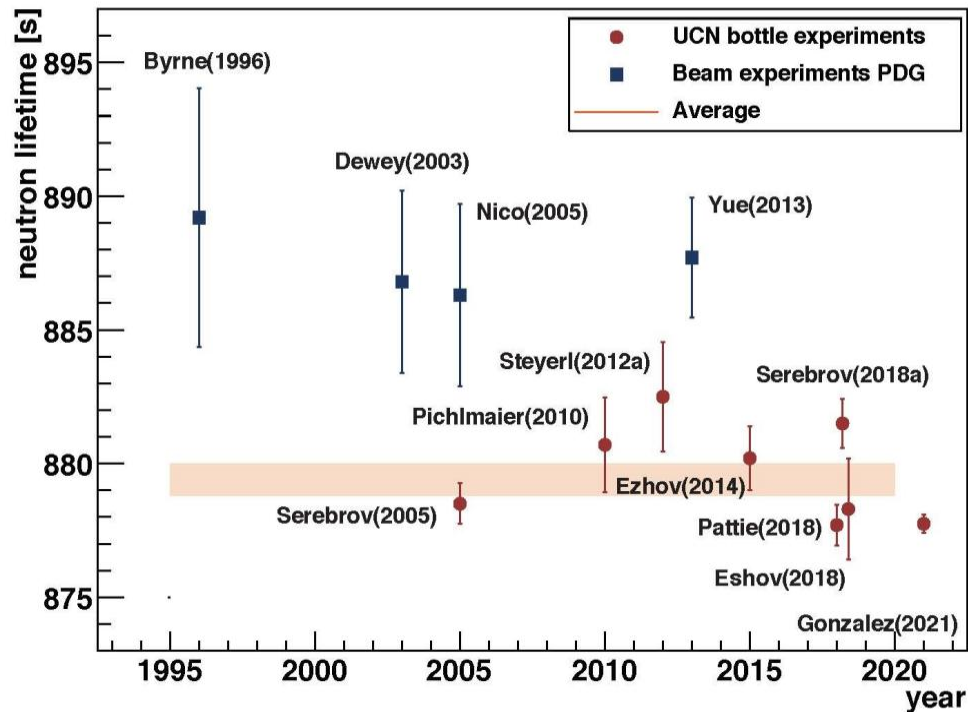
**Total reflection at all incident angles!**



**Can be stored until they decay!**

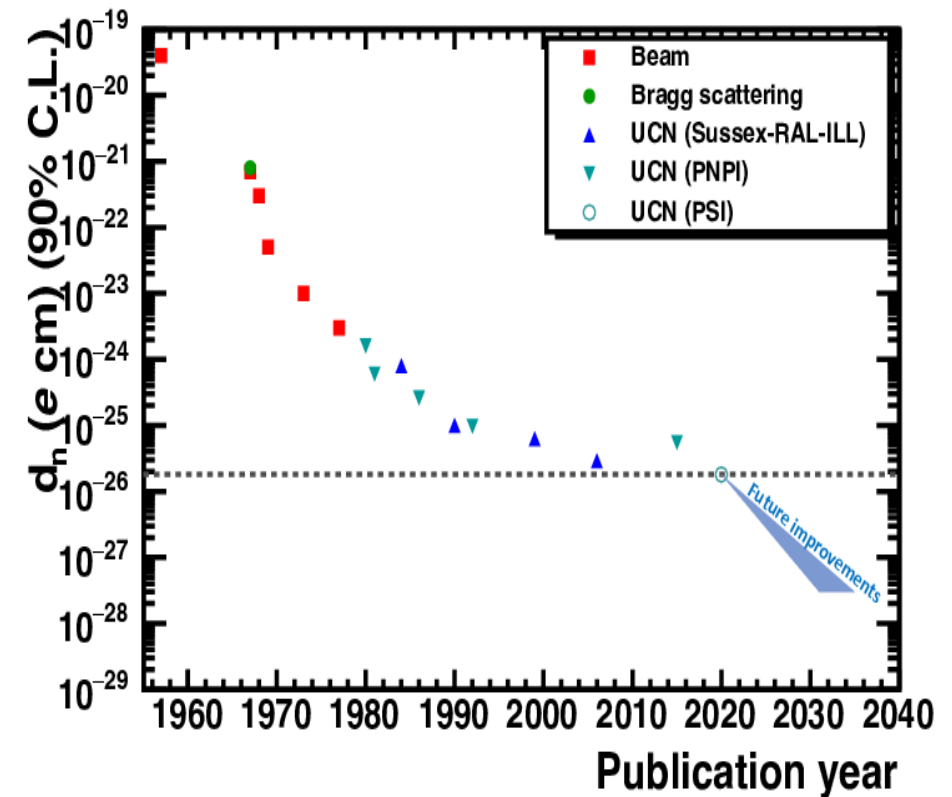
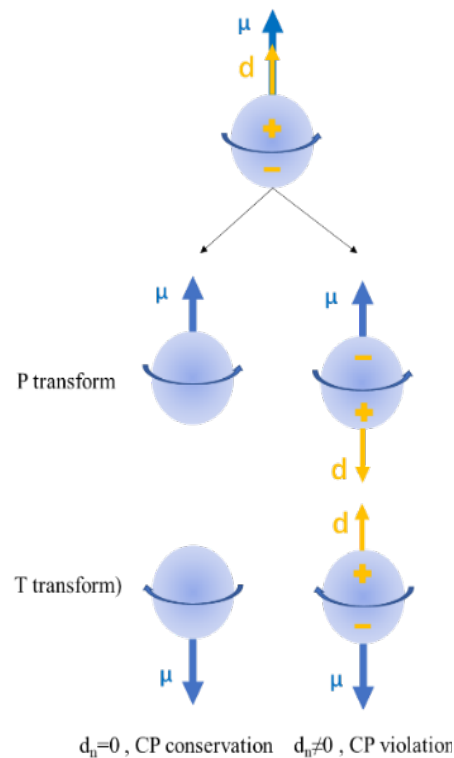
**UCN  
Features**



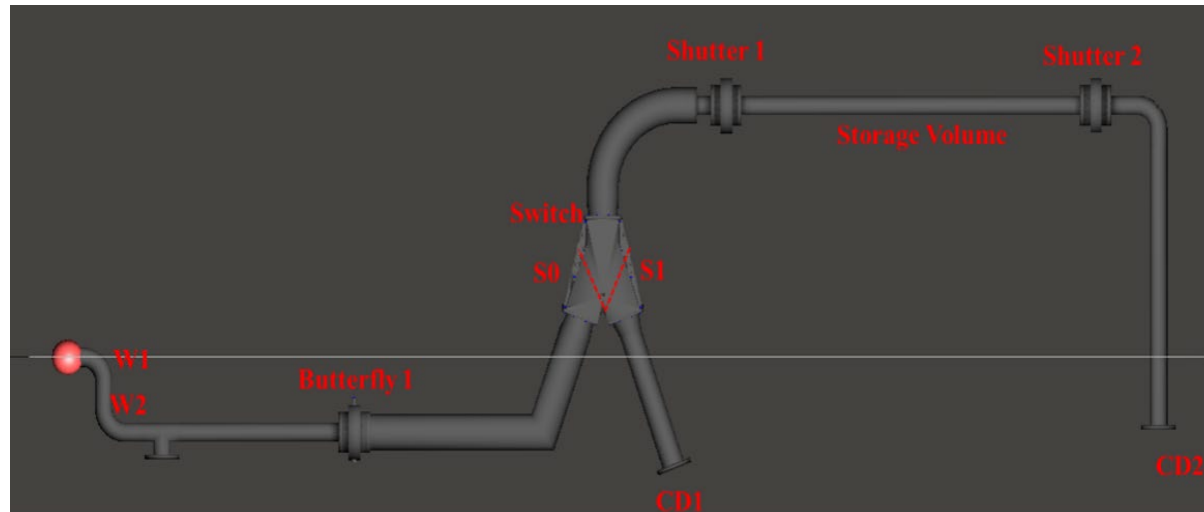


Neutron lifetime measurement history

(plot provided by Paul and Picker)

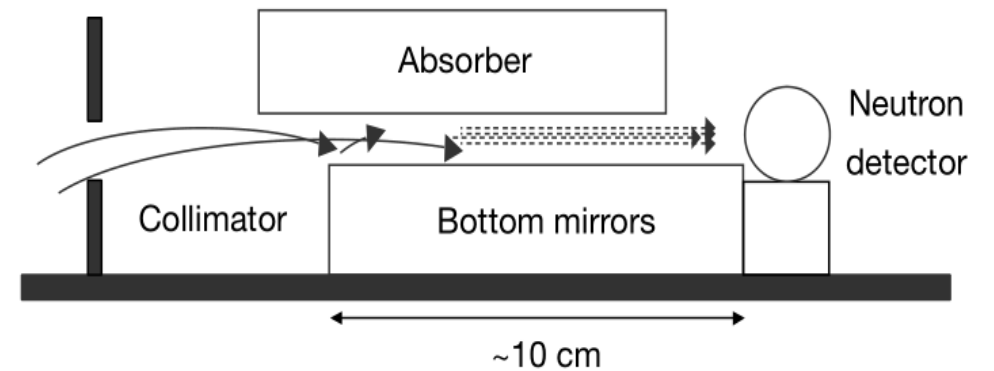


nEDM measurement history



UCN storage experiment

## Experimental Schematic for Measuring Neutron Energy Quantization in a Gravitational Field



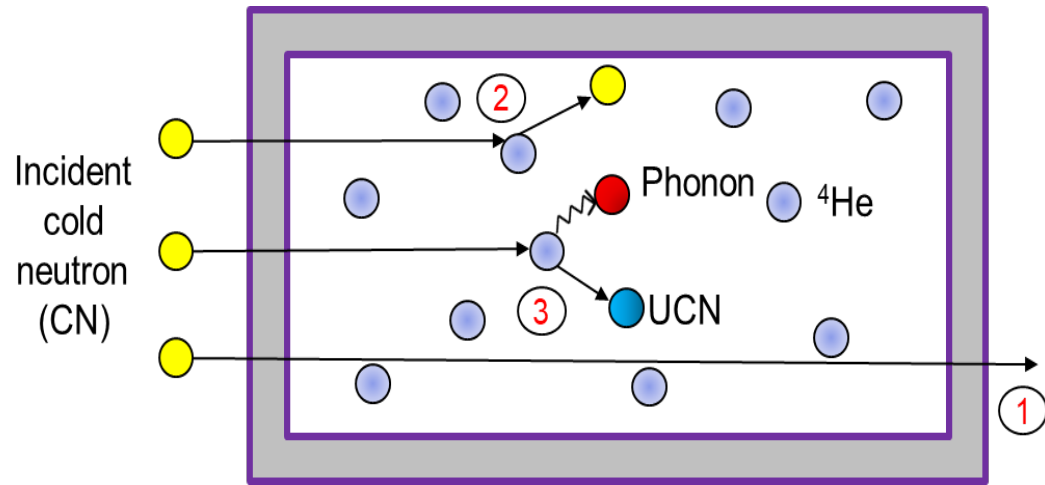
$$E_n = (\hbar^2 \mu g^2 / 2)^{1/3} \lambda_n, \quad n = 1, 2, 3, \dots$$

$$E_1 = 1.41, \quad E_2 = 2.46, \quad E_3 = 3.32, \quad E_4 = 4.08, \dots$$

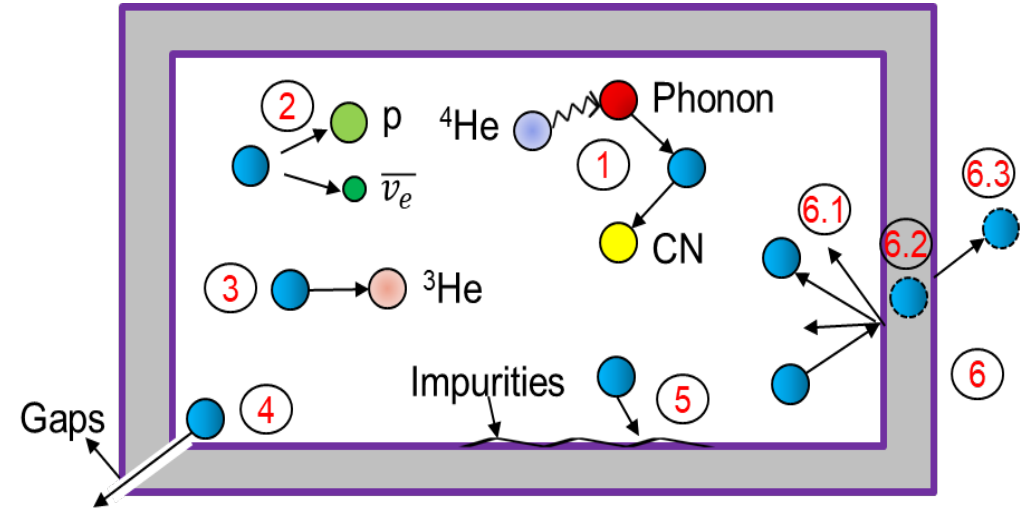
Unit: peV =  $10^{-12}$  eV

1. Background of UCN
2. Physical model enhancement and flow of iMCUCN
3. Comparison of MCUCN, iMCUCN, and UCNtransport
4. Comparison of MCUCN, iMCUCN, and experimental results

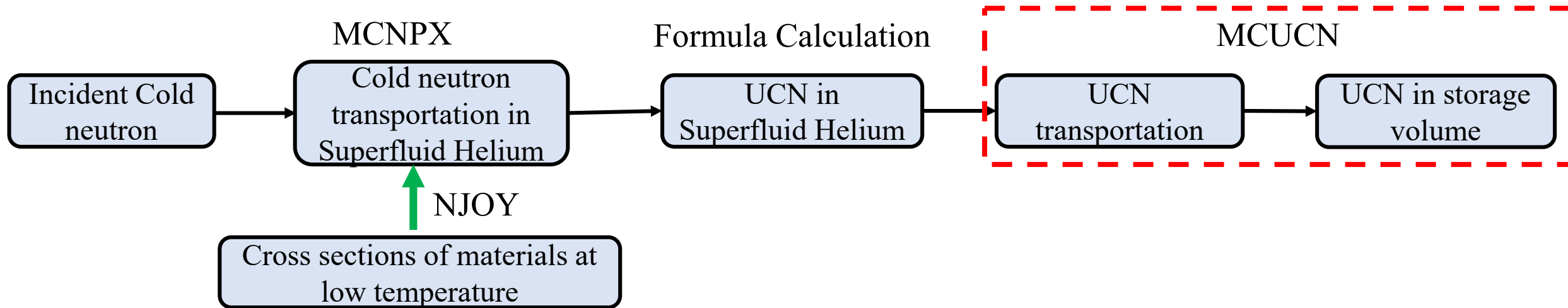
# The flow of UCN source design



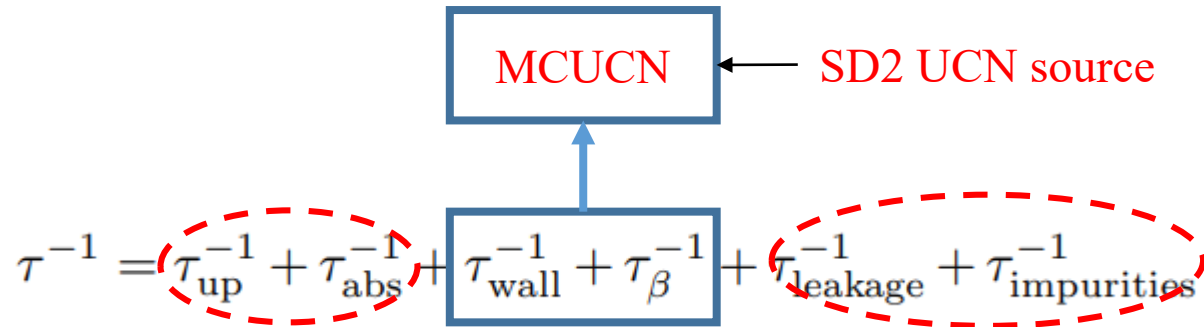
Cold neutron  $\rightarrow$  UCN



UCN storage and transportation



# The reason to improve MCUCN

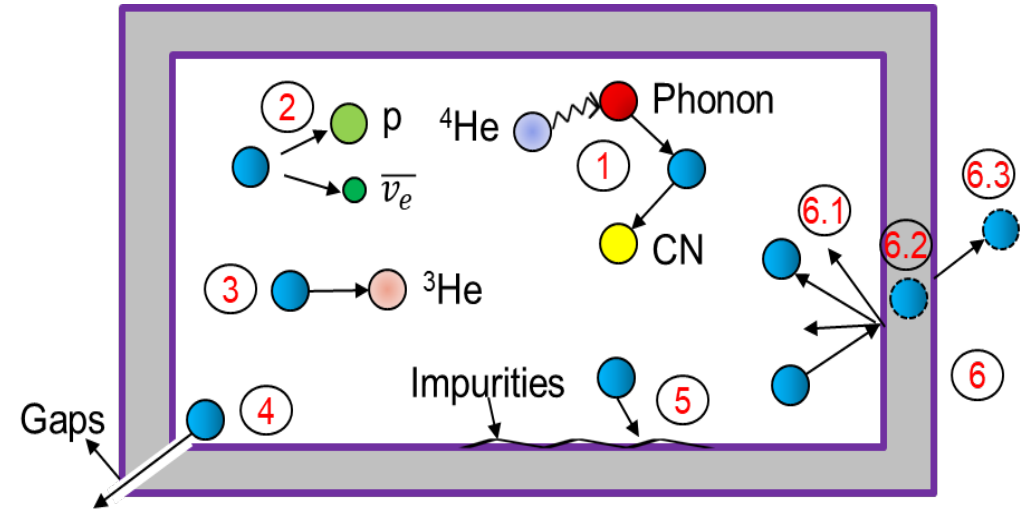


$$\frac{1}{\tau_{up}} = Ae^{-\frac{12}{T}} + BT^7 + CT^{\frac{3}{2}}e^{-\frac{8.6}{T}}$$

$$\frac{1}{\tau_{abs}} = n^{3He}\sigma_a v = n^{3He}\sigma_{a(th)}v_{(th)}$$

$$\frac{1}{\tau_{wall}} = \frac{\bar{\mu}(E_{UCN})vS}{4V}$$

$$\frac{1}{\tau_{leakage}} = \frac{S_{gap}v}{4V}$$



UCN storage and transportation

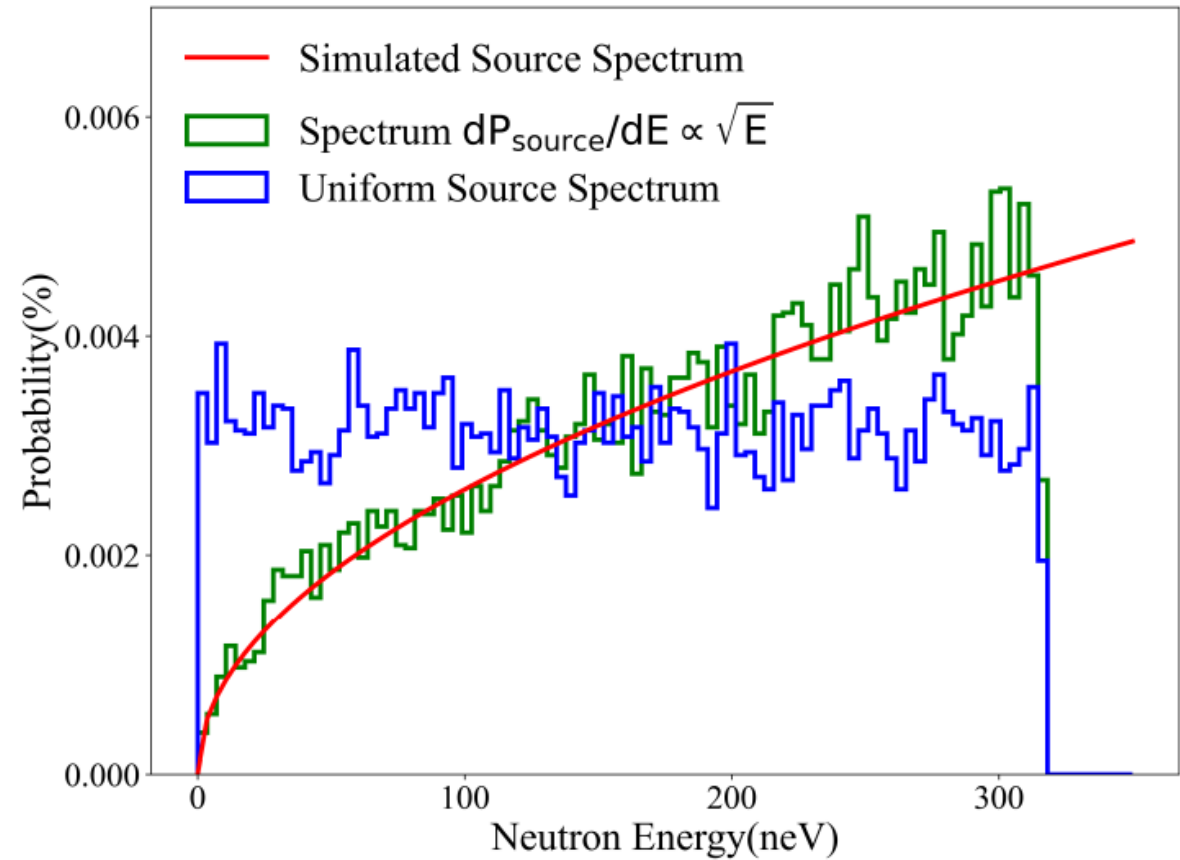
Material	$\sigma_{abs}$ (barn)	$\sigma_s/\sigma_a$	Optical penitential (neV)
$^4He$	0	$\infty$	18.5
$^2D$	0.000519	$1.47 \times 10^4$	105



$$\rho_{\text{real\_space}} d\epsilon_0 = \frac{d^3N}{d^3r} = \rho_{\text{phase\_space}} d^3p$$

$$\rho_{\text{real\_space}} d\epsilon_0 \sim p^2 dp \sim \sqrt{E} dE$$

$$dP_{\text{source}}/dE \propto \sqrt{E}$$



The normalized source UCN spectrum at different positions in the transport system. The red line stands for the formal expression  $dP_{\text{source}}/dE \propto \sqrt{E}$ . The green line is the UCN spectrum distribution in the UCN converter. The blue line is the uniform UCN source distribution in MCUCN.

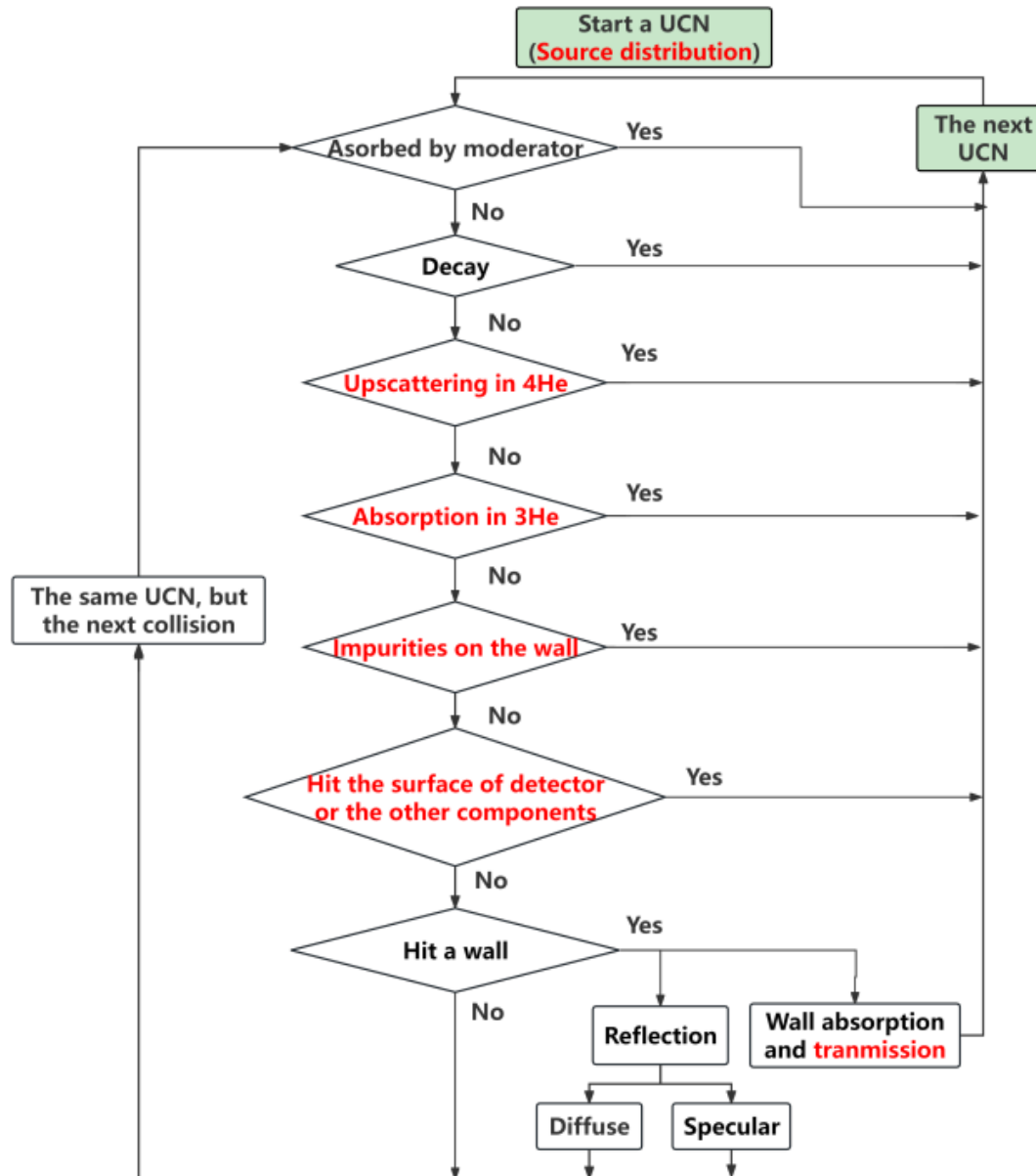
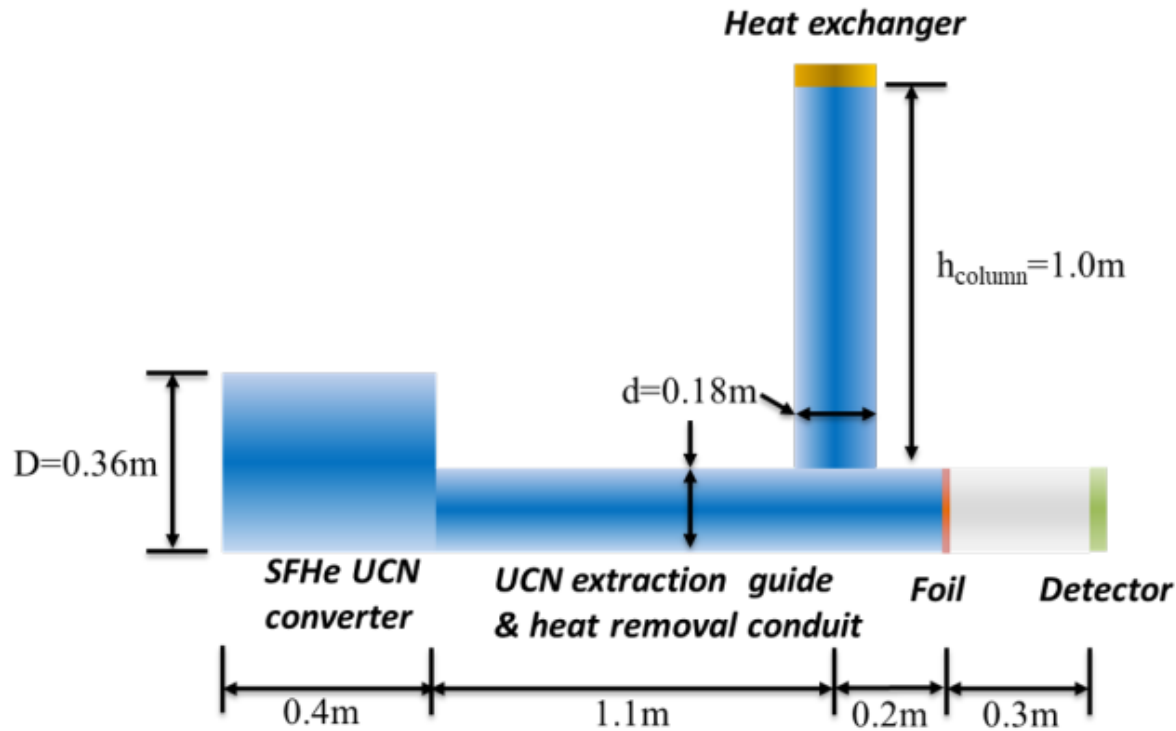


Illustration of the flow of physical models in the iMCUCN code. Diamonds indicate the physical models utilized for selecting a loss mechanism or going to exit window during transportation. Black characters represent original code sections, whereas our additions are highlighted in red

1. Background of UCN
2. Physical model enhancement and flow of iMCUCN
3. **Comparison of MCUCN, iMCUCN, and UCNtransport**
4. Comparison of MCUCN, iMCUCN, and experimental results

# Comparison of MCUCN, iMCUCN, and UCNtransport



The horizontal near-foil geometry of Lujan center Mark3 UCN transportation system

$$\tau^{-1} = \tau_{\text{up}}^{-1} + \tau_{\text{wall}}^{-1} + \tau_{\beta}^{-1}$$

Input parameters for the MCUCN and iMCUCN code sourced

Configuration	Parameters
Generated UCN number	10000
Detected UCN energy	$< 335\text{neV}(V_{58\text{Ni}})$
Cylinder	$D = 0.36\text{m}, L = 0.4\text{m}$
Radius of guide	$0.09\text{m}$
UCN Upscattering time	$3.4\text{ s (1.6K)}$
UCN decay time	880 s
$V_{\text{He}}$	18.5 neV
$V_{58\text{Ni}}$	335 neV
$\eta_{58\text{Ni}}$	$5 \times 10^{-4}$
$V_{\text{Al}}$	54 neV
$\eta_{\text{Al}}$	$5.19 \times 10^{-5}$
Diffuse rate of Al	45%
$V_{\text{PP}}$	-8 neV
$\eta_{\text{PP}}$	0
$\lambda_{\text{scat}}$ of idealized Al and PP	$0\mu\text{m}$
$\lambda_{\text{scat}}$ of PP	$20\mu\text{m}$
Thickness of Al and PP	$30\mu\text{m}$
Length of heat exchanger	1m
Loss of foil support grid	90%
4m guide loss to external volume	80%

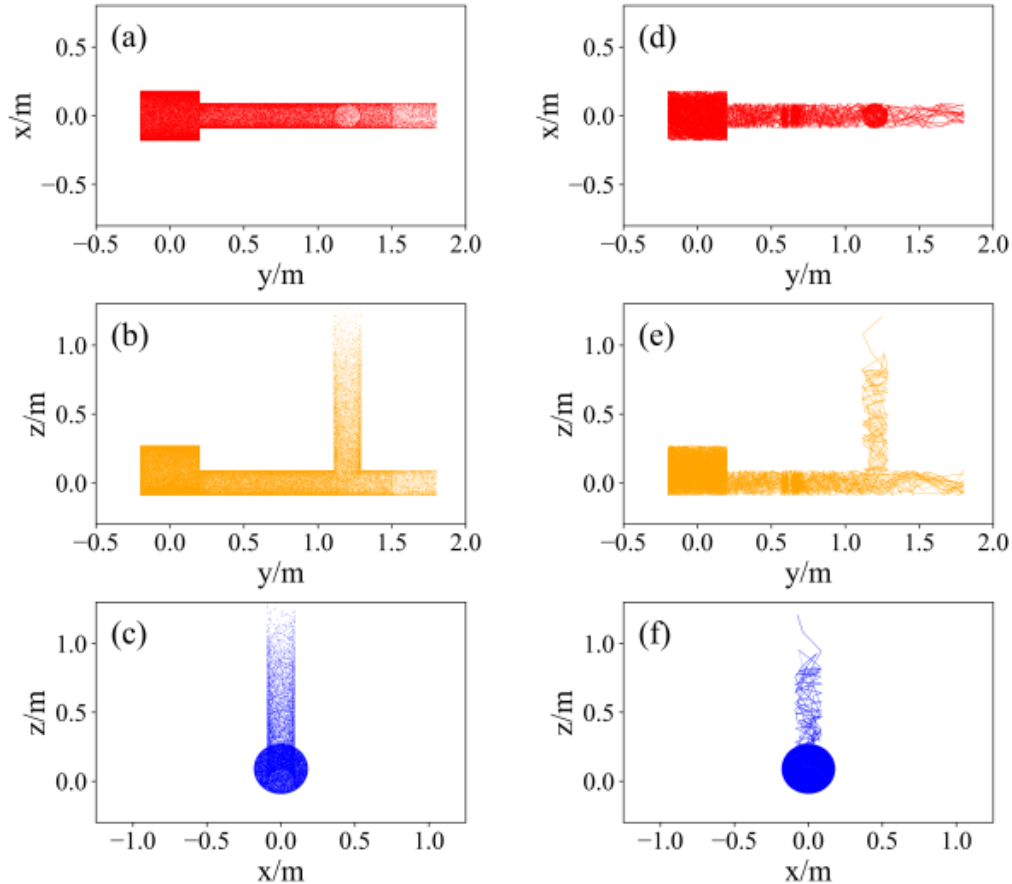
# Comparison of MCUCN, iMCUCN, and UCNtransport



Comparison of transmission rates simulated by MCUCN, iMCUCN, and UCNtransport

Configuration	T_MCUCN (%)	T_iMCUCN (%)	T_UCNtransport (%)	D (%)
Baseline: Al foil, $P_{\text{diffuse}} = 3\%$	66.6	34.1	35	2.6
$P_{\text{diffuse}} = 50\%$ in converter	72.6	42.1	43	2.1
$P_{\text{diffuse}} = 50\%$ in vertical volume	77.6	43.8	45	2.7
Switch foil from Al to ideal PP	85.5	49.3	53	7.0
Add PP elastic scattering	85.5	35.6	36	1.1
Add PP foil support grid loss	77.0	32.0	32	0.0
Add 4 m guide to external volume	61.6	25.6	26	1.5

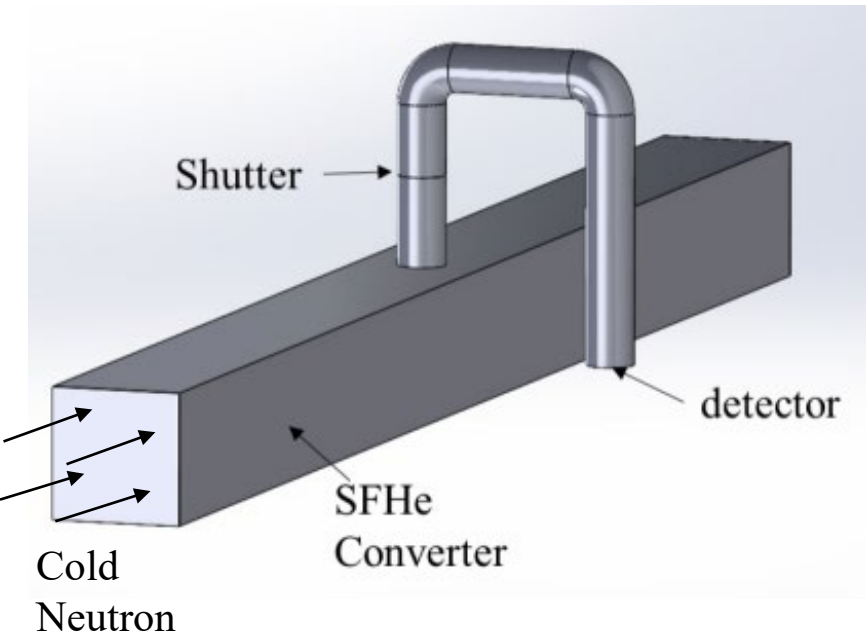
$h_{\text{column}}$ (m)	T_MCUCN (%)	T_iMCUCN (%)	T_UCNtransport (%)	D (%)
0.2	70.3	32.0	31.0	3.2
0.4	76.2	34.0	32.9	3.3
0.6	79.4	35.3	34.3	2.9
0.8	83.5	35.7	35.5	0.6
1.0	85.5	35.9	36.3	1.1
1.2	86.6	36.4	37.0	1.1



Added Geometry in the code and built the geometry.

Upscattering model in 4He is added in MCUCN successfully .

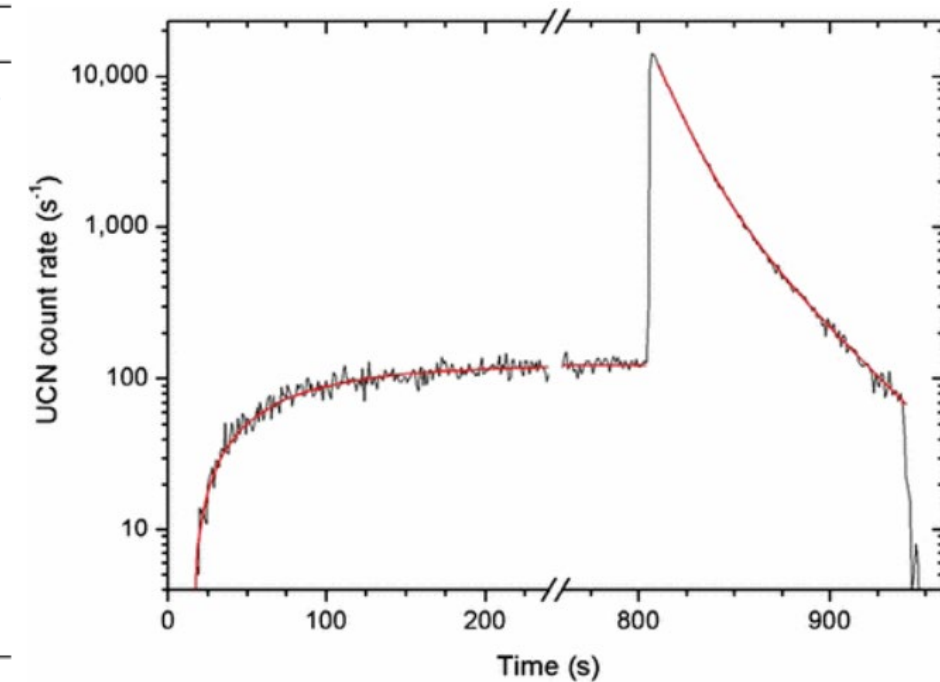
1. Background of UCN
2. Physical model enhancement and flow of iMCUCN
3. Comparison of MCUCN, iMCUCN, and UCNtransport
4. Comparison of MCUCN, iMCUCN, and experimental results



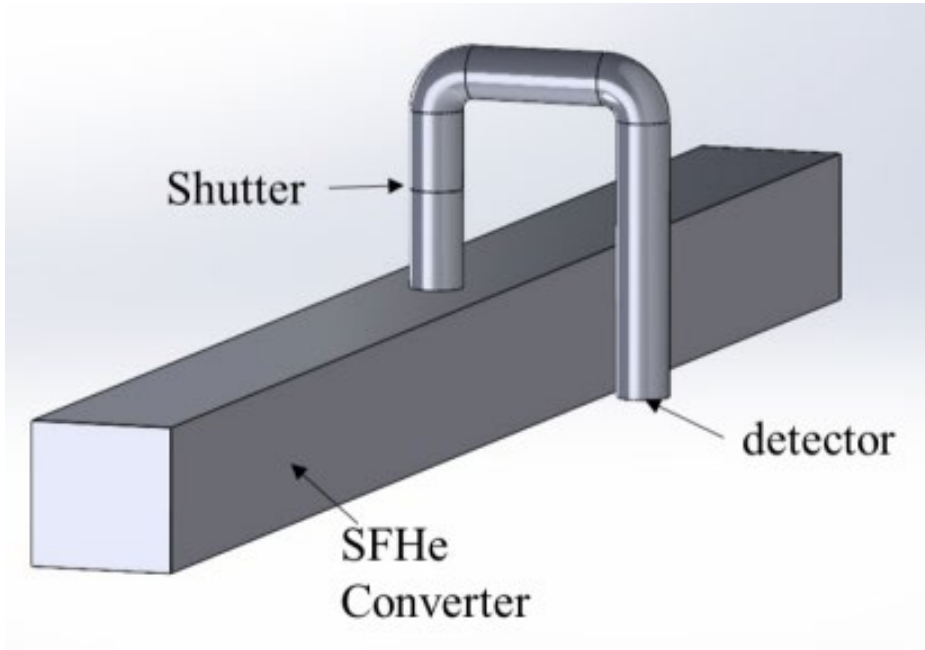
The geometry of SUN1

Configuration	Parameters
Converter	100cmx7cmx7cm
Radius of guide	0.0115m
$V_{\text{He}}$	18.5 neV
$V_{\text{BeO}}$	261.0 neV
$\eta_{\text{BeO}}$	$1.35 \times 10^{-5}$
$V_{\text{Be}}$	252.0 neV
$\eta_{\text{Be}}$	$5 \times 10^{-6}$
$V_{\text{stainless}}$	183.0 neV
$\eta_{\text{stainless}}$	$9.3 \times 10^{-5}$
Open shutter at	804 s
Close shutter at	937 s

Input parameters for the SUN1 experiment utilized in the simulation



SUN1 experimental results at detector.



The geometry of SUN1

Open shutter at 804 s  
Close shutter at 937 s

UCN number in the converter

$$N(t) = \rho(t)V = VP\tau \left(1 - e^{-\frac{t}{\tau}}\right) \quad N_{\text{sat}} = VP\tau$$

UCN count rate at the detector

$$C(t) = N(t) \frac{1}{\tau_{\text{leakage}}} T \quad T : \text{the transmission rate}$$

$$\frac{1}{\tau_{\text{leakage}}} = \frac{S_{\text{gap}}V}{4V}$$

$$C(t) \propto N(t) \propto \rho(t)$$

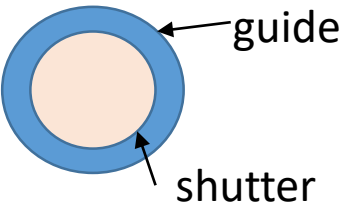
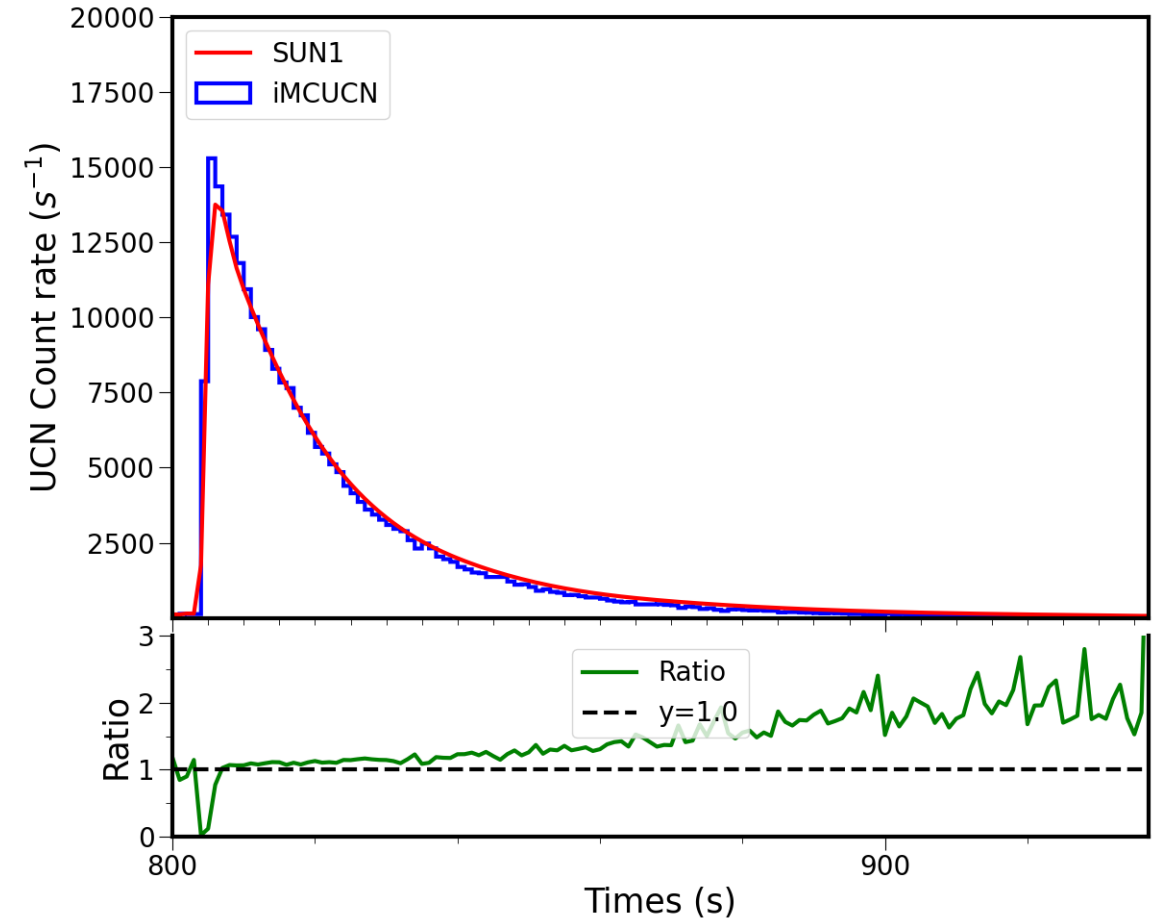
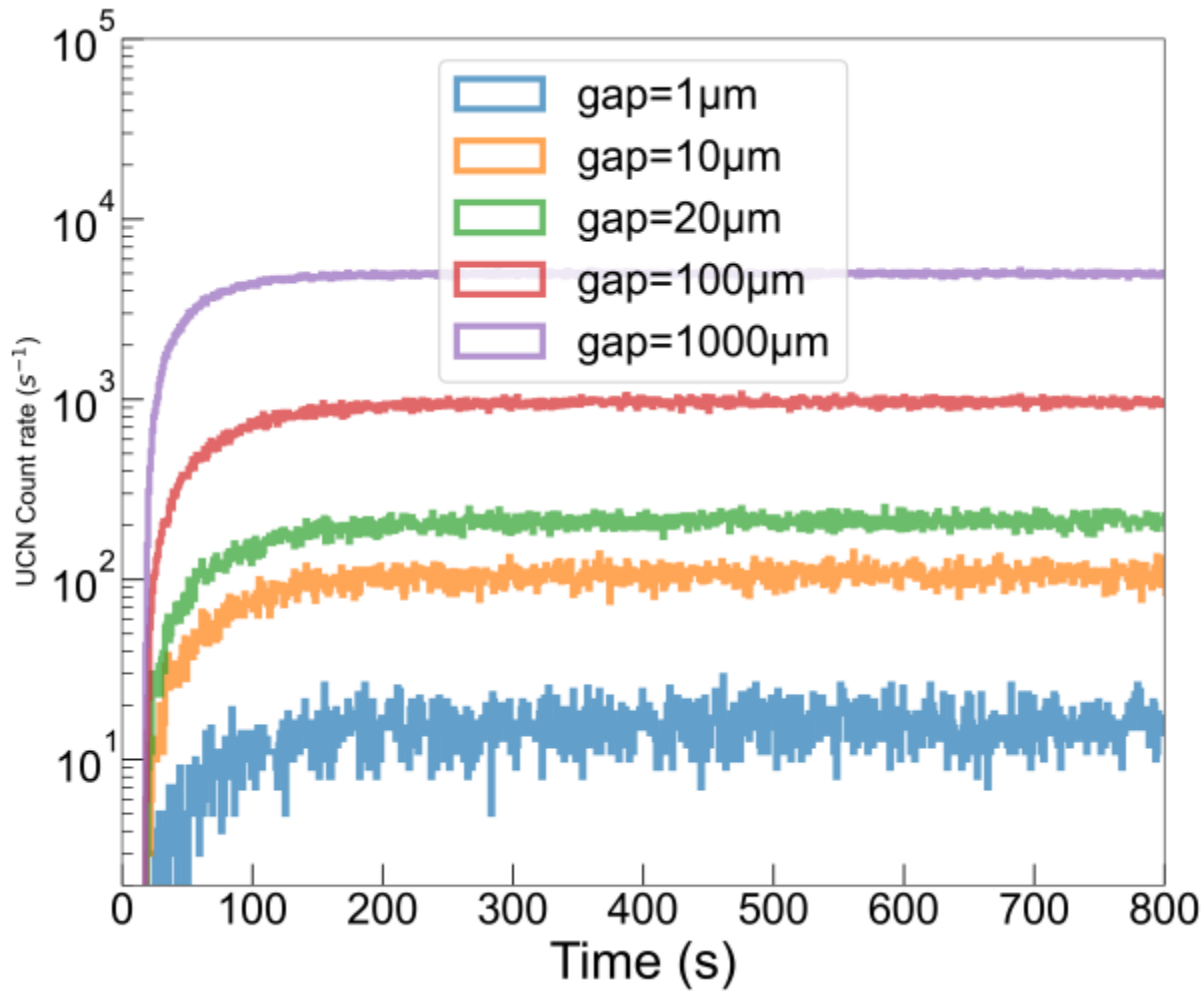
Before opening shutter,  $S_{\text{gap}}$  is the gap between the shutter and guide;  
After opening shutter,  $S_{\text{gap}} = S_{\text{guide}}$

$$\tau^{-1} = \tau_{\text{up}}^{-1} + \tau_{\text{abs}}^{-1} + \tau_{\text{wall}}^{-1} + \tau_{\beta}^{-1} + \tau_{\text{leakage}}^{-1} + \tau_{\text{impurities}}^{-1}$$

67s
1270s
315s
278s
880s
161s



# Comparison of MCUCN, iMCUCN, and experimental results



Fit the shutter gap, gap=24 $\mu m$   
 $S_{gap} = 0.017 cm^2$

To simplify the simulation, we assume that the losses caused by impurities and leakage are energy-dependent and adhere to the same regulation framework as wall loss

Buildup stage

$$C(t) = A \left( 1 - e^{-\frac{t-t_{\text{begin}}}{\tau}} \right)$$

Extraction stage

$$C(t) = B e^{-\frac{t}{\tau_1}} + C e^{-\frac{t}{\tau_2}}$$

The least square method :

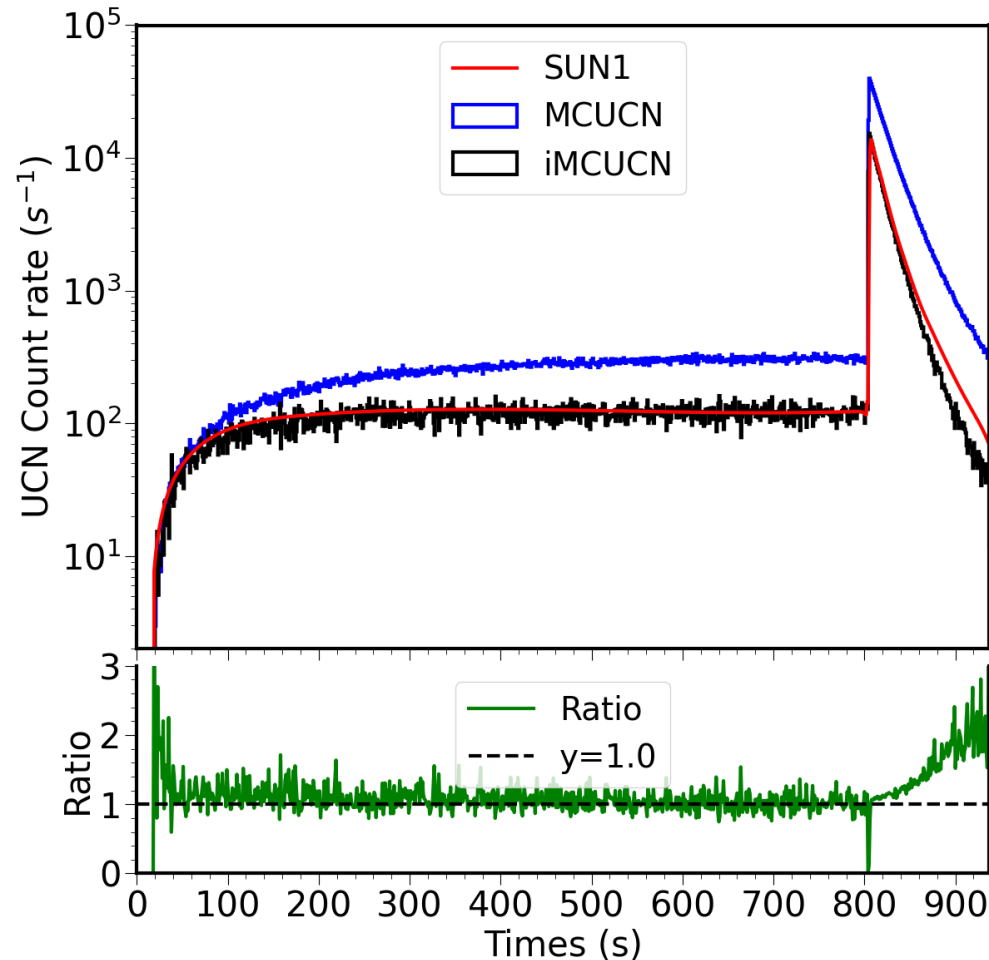
$$s = \left( 1 - \frac{\tau_1}{\tau_1(\text{experiment})} \right)^2 + \left( 1 - \frac{\tau_2}{\tau_2(\text{experiment})} \right)^2$$

The two decay time constants under different conditions

$d_{\text{guide}}(\%)$	$d_{\text{converter}}(\%)$	$\tau_1(\text{s})$	$\tau_2(\text{s})$	$s$
0.5	5.0	12.5	27.5	0.04
1.0	5.0	10.8	22.6	0.14
1.5	5.0	12.8	27.9	0.03
2.0	5.0	13.7	32.2	0.01
2.5	5.0	11.6	21.7	0.14
3.0	5.0	12.9	23.9	0.09
2.0	10.0	14.7	47.0	0.16
2.0	20.0	13.3	33.1	0.00
2.0	30.0	13.4	28.9	0.02

The final time constant

	$d_{\text{guide}}(\%)$	$d_{\text{converter}}(\%)$	$\tau$	$\tau_1(\text{s})$	$\tau_2(\text{s})$	$s$
SUN1	-	-	$67 \pm 3$	$13 \pm 1$	$34 \pm 1$	-
iMCUCN	2.0	20.0	<b>79.8</b>	13.1	28.4	0.03

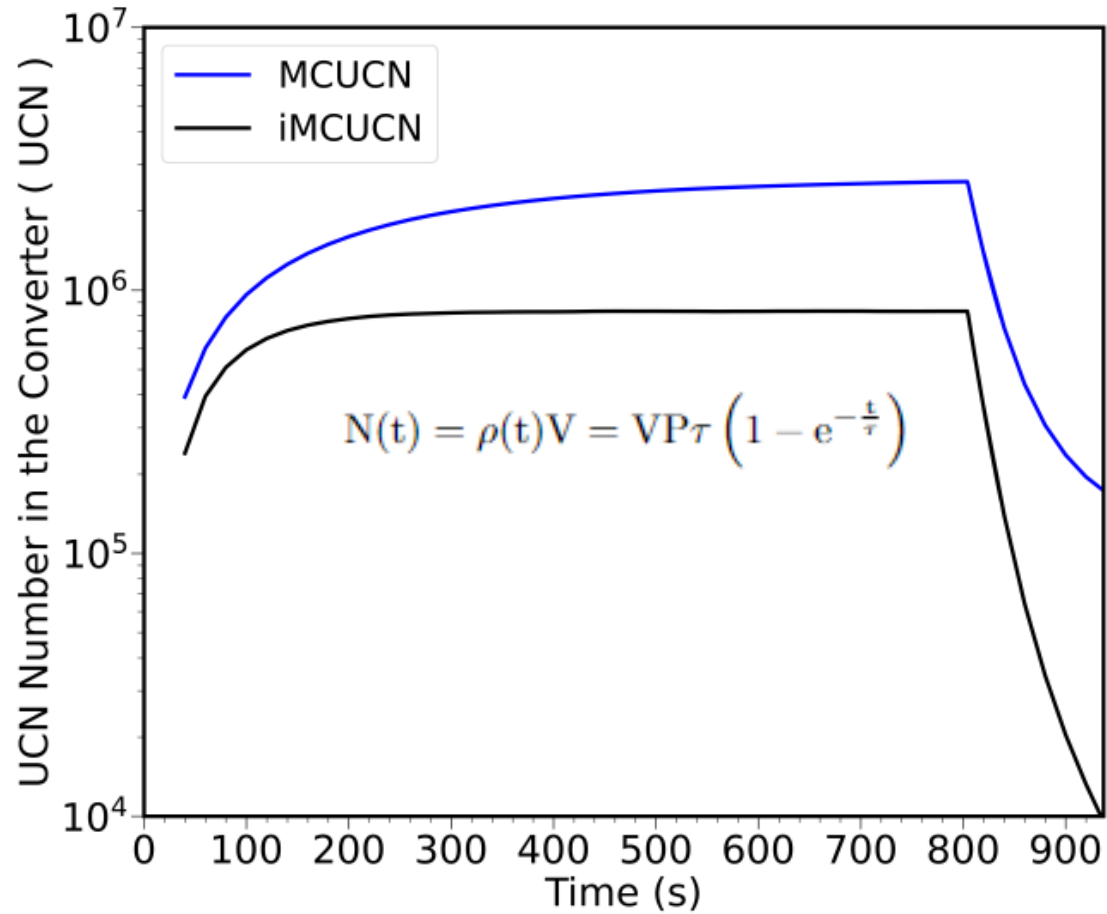


The discrepancy ranging from 840 s to 937 s between SUN1 measurements and data simulated by iMCUCN may arise from several factors.

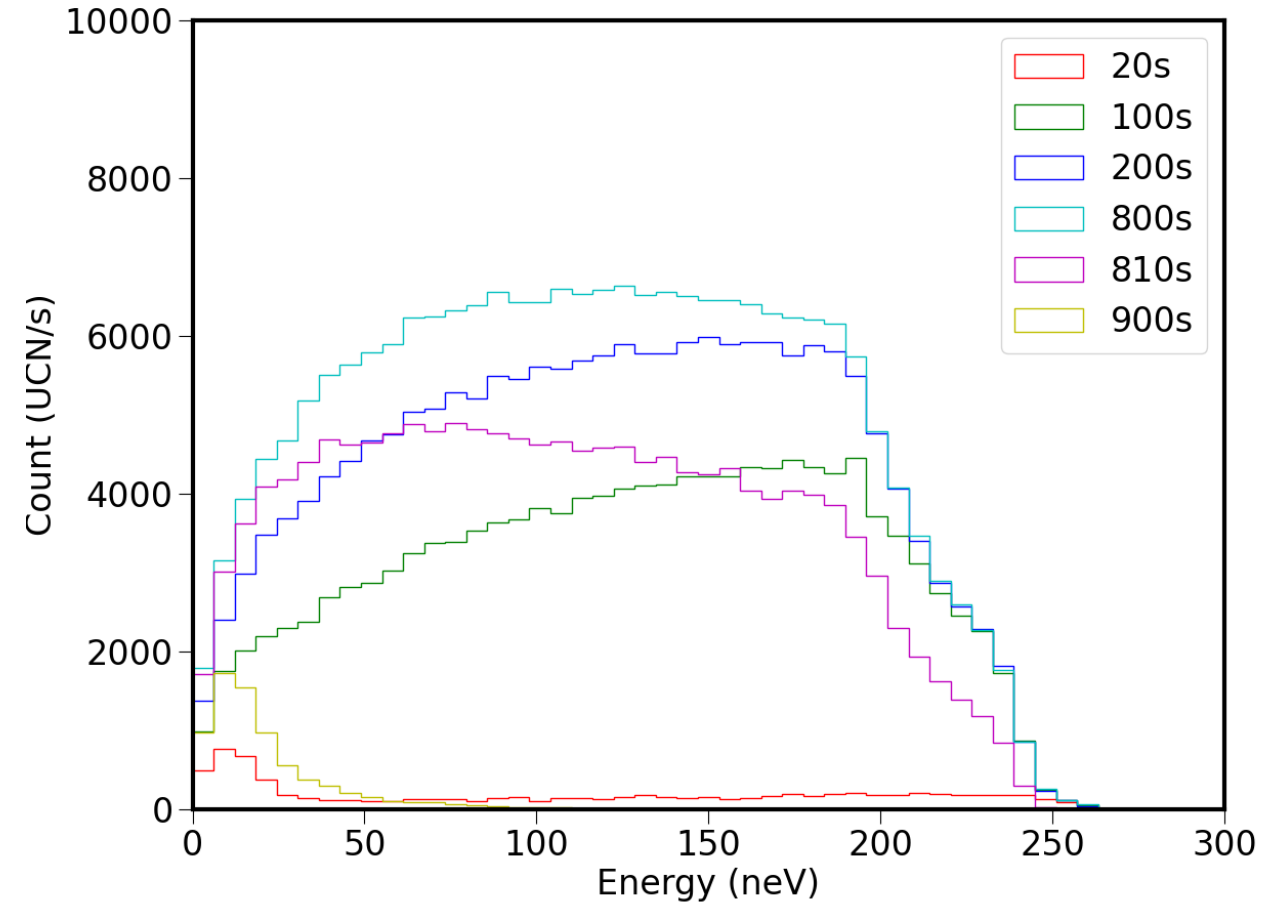
- (1) the UCN spectrum generated in theory may differ from the actual conditions in the experiment.
- (2) The energy-dependent loss mechanism rules of impurities and leakage rates can not be totally described by wall loss mechanism.
- (3) when the shutter is open, the leakage rate may also vary with UCN energy.
- (4) Furthermore, errors may be present in the data obtained.

As a result, the extracted spectrum is influenced by numerous specific reasons, which cannot be clearly explained at this stage. To clarify these discrepancies, further experiments need to be conducted.

To simplify the simulation, we assume that the losses caused by impurities and leakage are energy-dependent and adhere to the same regulation framework as wall loss



The UCN counts in the converter as a function of time simulated by iMCUCN and MCUCN.



The UCN spectrum in the converter as the change of time.

1. To enhance the MCUCN code, we performed several modifications, including:
    - 1) The incorporation of an  $4\text{He}$  upscattering physical model.
    - 2) The inclusion of a  $3\text{He}$  absorption model.
    - 3) The introduction of an impurities model.
    - 4) Improvements to the source energy distribution in SFHe and geometric description.
    - 5) The addition of transmission capabilities for materials with negative optical potential.
    - 6) Development of visualization tools for simulating intermediate states and results.
  2. Outline the physical models and flow of the iMCUCN code.
  3. Compare the results simulated by MCUCN, iMCUCN, and UCNtransport based on Lujan Center Mark3 UCN transportation system.
  4. Compare the results of MCUCN and iMCUCN with experimental data based on SUN1 UCN source.
- Consequently, iMCUCN is deemed valid and promising for UCN storage and transportation simulations in He II.



## The question I want to discuss



- (1) The UCN experiment demand for the UCN source.
- (2) Could we build one UCN source which fits for all the experiments?

Thank you for your attention!